

where d_1 is the beam diameter corresponds to the point where the irradiance (I_0) diminishes by a factor of $1/e^2$, and d is the radial distance of a point from the center, similarly, the thermal heat flux is modeled using equation (6) as follows:

$$q(r) = \frac{2P}{\pi r_0^2} e^{-\frac{2r^2}{r_0^2}} \quad (6)$$

where P is the laser power, r_0 the spot radius and r the radial distance. And the average heat flux on the laser spot is,

$$q_m = \frac{1}{\pi r_0^2} \int_0^{r_0} q(2\pi r) dr = \frac{0.865\alpha P}{\pi r_0^2} \quad (7)$$

where α is the absorption rate.

The laser beam distribution has been assumed to be either surface or volumetric in nature. To avoid the complexity, in [38] the powder has been considered to be a homogeneously absorbing and scattering continuum with effective radiation transfer properties equivalent to those of a powder bed. A surface laser beam is common in literature since there is not so much research on laser beam penetration [4,28,39, 38]. In [4], a ray tracing (RC) model has been formulated in which the geometry and structure of the powder have been taken into account. Figure 2 is the two-dimensional (2D) illustration of the model. As shown in figure 2, the laser beam is taken as the ray which penetrates into the powder bed, which is reflected and absorbed by the powders. This experiment was based on the simulation of a large number of rays. This model allows for calculation of the ratio of the total absorption with respect to the material absorption, laser beam penetration, and more. In [39], a volumetric line heat source has been considered with the energy characteristics shown as (8)

$$E_L = \frac{P_L}{v_s}, E_F = \frac{P_L}{h_s v_s} \quad (8)$$

where E_L is the line energy, E_F is the area energy, P_L is the laser power, v_s is the scan speed, and h_s is hatch spacing. In [28], a radiation transfer equation has been used with an isotropic scattering term to describe penetration in metallic powder. And in [7], it was concluded that if the finite element size is larger than five gradient diameters, laser penetration can be ignored in general.

Understanding of the interaction between the powder bed and laser beam is key to the laser penetration and powder bed absorption. Since the absorption parameter are not known accurately, in [16] a constant absorption ratio of pure titanium powder at the Nd-YAG laser wavelength (1.06 mm) was assumed. This assumption has been reported in [48] which also utilizes the absorption ratio for the bulk material. Similarly in [40, 41, 42] a constant absorption rate has been assumed in their modeling schemes. The laser energy absorptance of a material is known to depend on a number of factors such as the nature of the surface, level of oxidation, the wavelength of the incident laser beam, surface temperature, etc [43]. Though, in the case of metallic powders, the absorption ratio varies from the in-coupling absorption as proposed by Kruth et al [5] to within a few percent of the molten metal absorption ratio [20].

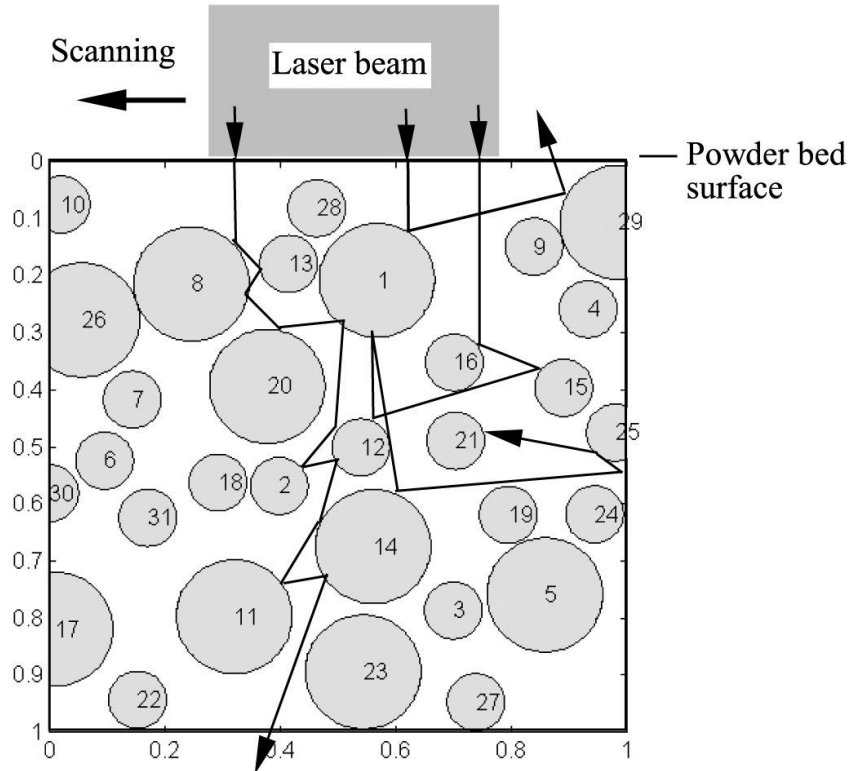


Figure 2 2D illustration of the RC model: simulation over a depth of 1mm and width of 1mm of powder bed [29]

Thermal properties include density, thermal conductivity, heat capacity and enthalpy. In [19], it was shown that thermal conductivity is not a constant value and seems to vary with temperature. In SLM, the effective thermal conductivity has been used. Many formulations were developed using reasonable assumptions or experimentation and it has been established that the powder bed porosity influences conductivity. The effective thermal conductivity is a function of solid and gas thermal conductivity [1,16, 75]. In [1], using the Yagui and Kunni (1989) function, the thermal conductivity of the material k_e has been expressed as (9)

$$k_e = \frac{\mu k_s}{1 + \Phi \frac{k_s}{k_g}} \quad (9)$$

where k_s is the conductivity of the solid material, k_g is the conductivity of air, μ is the solid fraction ($\mu = \frac{\rho}{\rho_s}$) and Φ is an empirical coefficient.

In [44], it has been proposed that thermal conductivity depends on porosity and pore geometries and it is controlled by the amount of gas content inside the pore. In [45], during their studies on light extinction in powder beds, it has been demonstrated that the effective thermal conductivity of a powder is essentially independent of material but depends on the size and morphology of the particles and the void fraction, as well as on the thermal conductivity of the gaseous environment. In [16], it has been established that the thermal conductivity of Ti6Al4V starts off from a low conductivity value for powder material and rises sharply at it nears the melting point. The thermal conductivity of this alloy increases considerably with temperature above room temperature. The temperature range near the melting point and above is the most important for the problem under consideration. In absence of any reliable experimental data, a constant value of $k_d = 20 \text{ W/(m K)}$ has been assumed, which is obtained by extrapolation to the melting point. The effective thermal conductivity of loose metallic powders is controlled by

gaseous content in the pores [28]. The density and heat capacity of alloy powder can be described as the mean of the individual components in [75].

Analytical solutions

The Carslaw and Jaeger [19] heat transfer model discussed above includes the unusual boundary conditions, and there is no analytical solution which completely satisfies the linear governing equation. However, there are some solutions associated with the simplified model which were first used in welding [46]. In particular, the Rosenthal solutions for a point and line heat source have been proved to be extremely useful in laser-based manufacturing.

The three dimensional (3D) Rosenthal's point solution for temperature distribution using a steady state point heat source moving on the surface of a semi-infinite plate along the x axis is given by (10)[2]

$$\bar{T} = \frac{e^{-(\bar{x}_0 + \sqrt{\bar{x}_0^2 + \bar{y}_0^2 + \bar{z}_0^2})}}{2\sqrt{\bar{x}_0^2 + \bar{y}_0^2 + \bar{z}_0^2}} \quad (10)$$

where

$$\bar{T} = \frac{T - T_0}{\left(\frac{\alpha Q}{\pi k}\right) \left(\frac{\rho c V}{2k}\right)}$$

$$\bar{x}_0 = \frac{x_0}{2k/\rho c V}, \bar{y}_0 = \frac{y_0}{2k/\rho c V}, \bar{z}_0 = \frac{z_0}{2k/\rho c V}$$

The 2D Rosenthal's line solution for the temperature distribution using a steady state line heat source moving on the surface of a semi-infinite plate along the x axis is given by (11)[47]

$$T = T_0 + \frac{Q}{k} \text{line}(x', y') \quad (11)$$

where

$$\text{line}(x', y') = \frac{1}{2\pi} \exp(x') K_0(\sqrt{x'^2 + y'^2})$$

$$x' = \frac{Vx}{2k}, y' = \frac{Vy}{2k}$$

and $\alpha, Q, V, \rho, c, k, K_0$ are the absorption rate, laser power, scan velocity, density, heat capacity, thermal conductivity and the modified Bessel function of the second kind and order zero.

The Rosenthal's solution plays an important role in the study of SLM temperature distribution. A more complicated solution for different laser beam distributions can be built upon these elementary solutions. In [46], the temperature distribution of a moving Gaussian distribution heat source has been derived. The influence of beam diameters has been included, though the solution was in the form of an integral and not a closed form solution. These scenarios can be extended to cover time dependent situations. The one-dimensional (1D) form of a time dependent point and line solution is derived in [47]. In [48], an expression of temperature distribution for a Gaussian heat source in a laser deposition process by using a Green function has been provided. Also, an analytical closed form solution for the maximum temperature of a stationary laser beam, an extremely fast moving laser beam and a laser beam with intermediate velocity has been derived. In [49], a semi-analytical model has been

developed to estimate the thermal field created at a sample surface during a pulsed Nd-YAG laser treatment with constant thermal properties and a laser beam with Gaussian distribution. In [18], equation (1) has been solved analytically with boundary conditions provided in equation (4), the solution strategy ignores other important boundary conditions, such as convection, radiation, etc. From the literature, there are no analytical solutions for the complete problem without considering the nonlinearity of the thermal properties. There are some of the closed form analytical solutions such as the Rosenthal solution for very simple problems. The closed form solution transforms into an integral for more complex boundary conditions. Although these analytical or semi-analytical solutions are very important in the thermal study of SLM, they have many limitations. These solutions, though simple, can help lead to a better understanding of the problem before resorting to more complicated computational methods [47]

Numerical Solutions

Numerical methods are generally used for solving complex problems when closed-form solutions are not available for a physical situation. A number of research groups have reported their simulation strategies and results in the literature and are enumerated in Table 1. . The simulation strategies can be classified by model dimensions, linear/nonlinear approaches, substrate characteristics and laser beam characteristics. The computation time for a real comprehensive model which considers all the factors above is very large and it takes hundreds of hours to compute a 3D model with several layers of real-time SLM processing.

Table 1: Summary of simulation model from literature review

Reference	Material	Basement	Model size: mm	Element size: mm	Laser popup: w	Scan speed: mm/s	Hatch space: mm	Laser beam: mm	Laser type
50	Nickel alloy	N	1.6x(5,10,20)x3.75	0.25	1000	4	0.75	0.75	N/A
51	titanium	N	0.1x0.1	12.5e-3	2	1	N/A	50e-3	Gaussian
7	titanium	N	Coarse: 5x5x2	Coarse:0.1	2	1	0.1	25	N/A
			Fine: 2x2x0.5	Fine:0.01					
40	Cu	N	Height:10	N/A	50-2500	N/A	N/A	0.8	Uniform
52	iron	N	0.03x0.9x0.9	7.5e-3	2,3,4	180,200,225	0.0225	0.03-0.06	Gaussian
8	W-Ni-Fe	Metal: 2x3x1.5	1x2x0.05	0.05	100	20-140	0.05-0.15	0.05	N/A
16	titanium	Mild steel: 3x3x3	1x1x0.15	0.025x0.025x0.03	120	220	N/A	0.1	Gaussian
41	copper	4.8x2x0.5	3.4x1.6x.3	0.1	400	60,120,180	0.3	0.4	Gaussian
53	H13 hot work tool steel	mild steel	20x20x9	N/A	80	500	N/A	0.1	N/A
42	titanium	stainless steel 25x10x5mm	2x1x0.05	5e-3	110	200	N/A	0.034	Gaussian

29	42CrMo4	100x50x5mm	N/A	17675 elements	3500	10-30	N/A	Wide band:10x8 3x1	Rectangular
30	ceramic	N	20x24x2	0.2	10	3.3	N/A	2	Gaussian

The finite element (FE) and finite difference (FD) methods are the most commonly used numerical methods for solving the SLM thermal problem. A 1D model has its advantages for saving computation time and an ability to reflect some of the main characteristics of the SLM thermal problem. Henceforth, it has been employed commonly in the literature. In [54], a 1D FE model has been developed to simulate the SLS process using Bisphenol-a polycarbonate, and the solution was determined using a basic feed forward FD method. In [40], the axisymmetric heat conduction problem involving the melting of Cu with a pulsed laser source has been solved using a traditional backward difference scheme and Galerkin's FE formulation. The FE mesh has been reconstructed from the change of molten pool shape. In [28], a single line scan on a layer of unconsolidated steel 316L powder has been studied by considering other heat transfer mechanisms such as the radiation and convective heat transfer. The temperature distribution of a single track of laser scanning on the Ti6Al4V powder was studied by including the temperature dependent thermal conductivity and heat capacity in ANSYS [42]. In [29], the thermal field of a wide band laser heat source scanning a single track has been studied and the heat source is considered volumetric.

The 2D model is extensively developed and discussed. A 1D model is not always enough to explore the details of the thermal properties. The 2D model is not as time-consuming and expensive to produce as 3D, and keeps more details than the 1D model. So the 2D model is often appropriate and useful. In [1], the temperature field is described by a quasi steady state equation which has been numerically solved by using the stream upwind Petrov Galerkin (SUPG) strategy together with a shock capturing scheme. In [50], a 2D FE model for a single nickel layer formed on the powder bed by SLM has been derived through the Galerkin method with the backward difference scheme. In [7], the FE method for space discretization coupled with a Chernoff scheme for time discretization, which was proved in [55] that this method provides a fully converged solution to the model, is employed to predict the temperature distribution on the top surface of a titanium powder bed during laser sintering of titanium powder. The quasi regular mesh with fine laser spot area cells and coarse cells in neighbor areas was employed to relieve the computation burden. [56] reports a FE model to simulate the temperature field of polymer-coated molybdenum powder in the SLS process. The model was solved using FORTRAN with fine and coarse meshing. The relative error between the experiment and numerical simulation results were less than 5%. In [51], a 2D non-linear heat transfer with volume internal heat source problem is numerically solved based on the coupling of Matlab and ANSYS FEM models. The phase change effect, effective thermal conductivity, heat capacity and the Gaussian laser energy as internal heat source were considered in this model. The model was spatially discrete by Galerkin FE formulation and time discrete by implicit FE method. [8] predict the surface temperature distribution during SLM of 90W-7Ni-3F materials. [52,53,30] report their research results of temperature fields in single metallic layer SLM processes by using element birth and death.

The 3D model is able to better reflect the real SLM process and provides more information about the thermal field. In [39], a macroscopic FE-model using three different geometries and a volumetric line heat source has been presented. The 3D model shows the sintering of a single line, whereas two dimension models are used for longitudinal and crosscuts

of the sintering process. In [16], a more comprehensive understanding of the SLM thermal field has been achieved by creating a 3D model and considering the interval time (1s) for new powder recoating. A 10% convergence test was conducted to ascertain the suitability of the chosen mesh divisions. In [41], the substrate is included into a 3D thermal model which has three layers of powder. In [57], it takes several hours to simulate a 0.6x0.5x0.5mm cuboid using ABAQUS. It was concluded that using 2D analysis with generalized plane strain conditions seems to be convenient, but 3D analysis remains absolutely necessary to full understand the problem.

Thermal measurements

Analytical and numerical models have limitations when predicting the thermal field in SLM since assumptions are necessary to simplify the problem. These models help researchers understand the process, however, to comprehensively understand the SLM thermal problem, measurements of temperature distribution during SLM are needed to validate the assumption and results. Experimental temperature measurement helps to better understand the interaction between the laser beam and powder bed [5]. Thermal imaging methods have been used numerous times for the determination of temperatures and the results have been published in different papers and theses [7,16,56,58,59,60]. However, the system is affected by the distance of the infrared device and powder bed. [7,16,56,59,60] set up the temperature measurement system to compare and validate their simulation model result by using an infrared camera. The top surface average temperature of titanium powder was measured in [59] under the continuous and pulsed wave modes of an Nd:YAG laser. The results show that the average powder bed surface temperature using pulsed wave mode is 30% lower than the continuous wave mode. Also, consolidation in pulsed wave mode is much more efficient than continuous wave mode. However, cameras were not able to resolve the temporarily higher skin temperature rises. The same experiments were carried out [7] for titanium powder. Temperatures less than 500 °C were not presented since the camera data was not reliable below that threshold. The infrared camera resolution used in [7,59] was 256x256. [56,60] build an infrared thermometer to measure the powder surface temperature, and use the thermocouple to test the interior temperature of polymer-coated molybdenum powder in the SLS process. However, [7,56,59,61] do not describe details of their systems like implementation, camera angle, etc. In [58], a temperature monitoring system for a laser sintering system is presented and it explains the importance of the angle between the camera's axis and surface normal. Some reference papers in [58] from Europe analyze the influence of this angle and experiments have been done to measure the temperature using different angles. For this experiment a thermal imaging system was built into a DTM Sinterstation 2500. The thermal system uses the InfraTec Jade III MWIR with an optical resolution of 320x240, which is able to measure the whole powder temperature and also the melting temperature of the molten pool.

[62,63,64,65] develop feedback temperature control systems to ensure a homogenous temperature field and stable molten pool. A CMOS camera based control loop system is used in [62] to measure the melt pool size and control for overhanging structures. The controller bandwidth was only applied to limited scan velocities. [63,64] improve the controller to be able to monitor the melt pool continuously at high speed through the building process in real time. The thermal monitoring system was a combination of two types of optical sensors – a 2D digital CCD camera and a single spot pyrometer based on photodiodes [65]. Both monitoring systems were developed and used for the SLS/SLM process according to their different laser spot sizes.

Process parameter effects and optimization

The quality of laser sintered parts greatly depends on proper selection of the processing parameters, such as laser power, scanning speed, spot size and material. These have significant influence on the temperature distribution in the powder bed. A homogenous temperature field can lead to better microstructure, mechanical properties, dimensional accuracy and surface finish. Researchers typically try to find a relationship between process parameters and the temperature field. Simulation models and design of experiment methods are the two most common ways to evaluate effects and correlations. The simulation results from [8,41,52,66] conclude that the peak temperature will increase with higher laser power and lower scan speed. These phenomena result from the increasing energy density corresponding to higher laser power and lower scan speed. T.C. Child and C. Hauser in [52,66,67] create a single track process map, shown in figure 3. The whole map is divided into five areas and each represents the 314SS single track shape with different laser power and scanning speeds. A preheating and narrower scan interval will increase the peak temperature [8]. In [41], the study shows that the surface quality of a single sintered layer will improve by lower scanning speed; however, higher scan speed is needed to improve the multi layer surface quality.

Experimental design methods are usually used to test the process parameter effects and predict the temperature using a database collected from experiment or simulation. Part density is predicted in [68] as a nonlinear function of several process parameters in SLM by response surface methods. The data is from a simulation model based on ANSYS. Central composition design is used in [69] to predict the density, hardness and porosity of sintered low carbon steel parts under a pulsed Nd:YAG laser. The design shows that increasing layer thickness and hatching distance results in an increase in porosity and decrease in the hardness and density [69]. [70,71] use EFCP²³ and central point to study how process parameters effect single tracks and single layers in SLM.

Classical design of experiment methods need a large numbers of data. Some advanced intelligence methods can make predictions using smaller databases. The neural network method is one advanced method from the literature [72,30]. In [64], it is used to build a model based on a feed-forward neural network (NN) with a back propagation (BP) learning algorithm. The basic idea is to train the prepared database first and then use the NN algorithm to create a good mapping between the process parameters and their resulting properties. Then the system can help to determine the most suitable process parameters automatically. In [73], an iterative method to optimize non-linear processes was developed. This neural model is able to make adjustment of the four process parameters with regard to target values of three product properties. The method is applied to SLM of titanium powder.

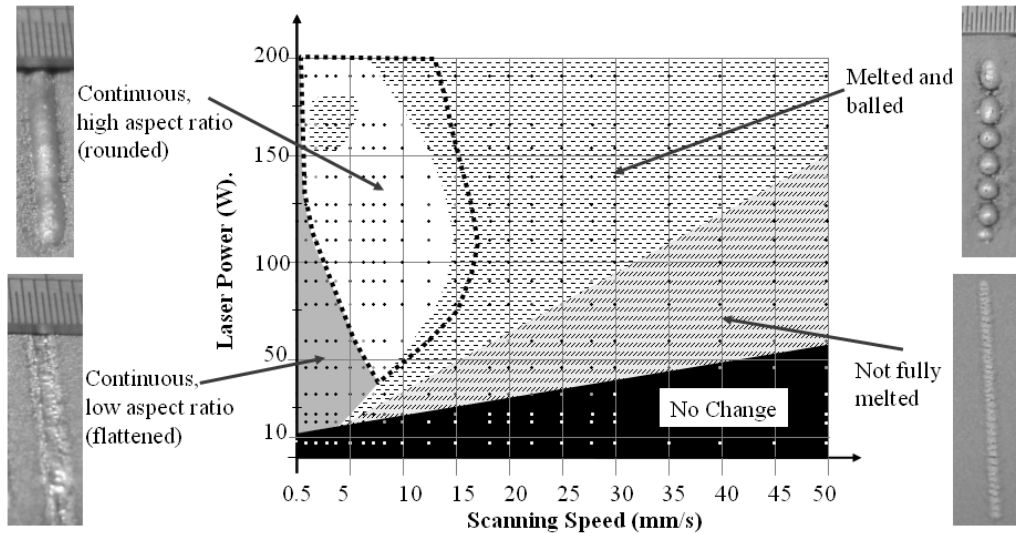


Figure 3 314S single track process map produced using a laser spot size of 1.1mm [52]

Case study

This section uses a model to show some characteristics of the SLM thermal field. The model in this study represents building Ti6Al4V on a Steel substrate, which is shown in Figure 4. The process parameters and Ti6Al4V thermal properties are adopted from [16]. The material is mild steel from [42]. The model and process parameters are shown in table 2. The simulation is carried out in ANSYS. The laser beam is assumed to have a Gaussian distribution with spot size 100 μm . The element size is one quarter of the laser diameter and the laser energy is distributed on a 4X4 grid at every load step. The scanning strategy is the traditional S pattern. Convective heat and radiation in the molten pool is neglected [16]. Laser power and substrate surface heat convection are considered and the initial temperature is set at 335K.

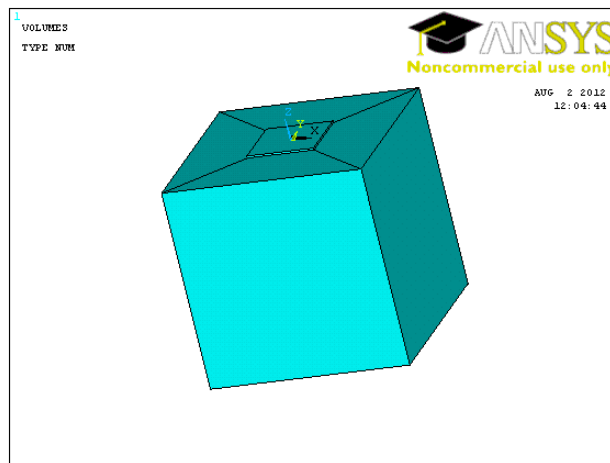


Figure 4. 3D model with substrate

The model simulates one powder bed layer. The temperature profile for the first layer is shown in figure 5, in which the scanning direction is from right to left. The temperature isotherm

curve is a series of ellipses, which agrees with the result in [8]. The contour plot also shows that the front end of the molten pool is denser than the back end, that is, the thermal gradient at the front of the molten pool is larger than the back when considering laser scan direction. The reasons are mainly because of the different material thermal properties since they are temperature dependent and the thermal conductivity is increasing with increasing temperature as well as the fact that the laser source is moving.

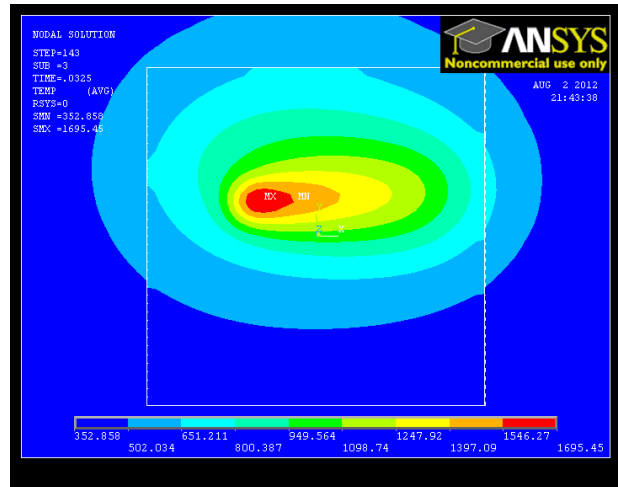


Figure 6 Temperature profile at 0.0325s

Temperature variation with time is shown in figure 7. Figure 7(a) shows that for one track scanning there is only one temperature peak. Figure 7(b) shows temperature variation for single layer scanning. There are three temperature peaks. The laser scanning is following a traditional S pattern as it scans back and forth. As such the laser will heat the same position three times per layer, which leads to rapid temperature increases and drops three times. The number of peaks is determined by the laser spot diameter and hatch spacing. From figure 7 can be observed that the temperature increase rate is higher than the cooling rate. One important phenomenon is that the peak temperature happens after the laser beam has passed the spot. There is a lag between the laser beam and peak temperature. The red line in figure 7 illustrates the time when the laser beam passes, and it can be seen that the peak temperature happens after the beam has passed.

Table 2 Model information and process parameters

Process parameters			
Laser power	120w		
Laser type	Gaussian distribution		
Spot size	100 μm		
Scanning speed	220mm/s		
Powder size	30 μm		
Hatch space	50 μm		
Absorption rate	0.35		
Model information			
	Material	Dimension(mm)	Meshing(mm)
Block	Ti6Al4V	3x3x3	free
Substrate	Mild Steel	1x1x0.03	0.025x0.025x0.03

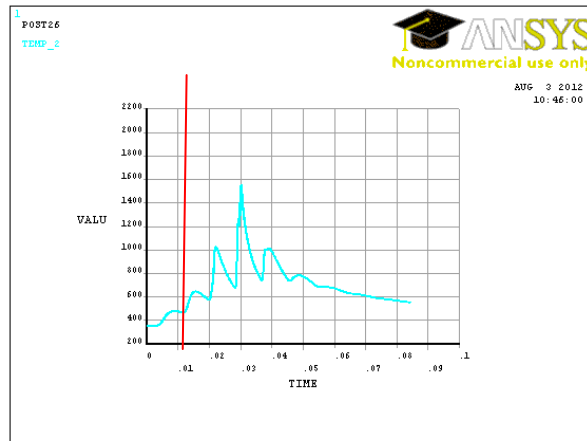
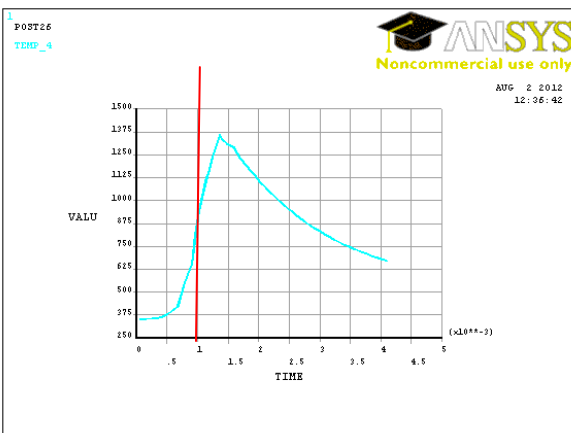


Figure 7 Temperature variation with time for one track scan (a), temperature variation with time for one layer scan (b)

The pictures shown in Figures 8 and 9 are the process parameter effects of laser power and scan speed. The peak temperature increases with higher laser power and lower scan speed which has been shown in [8,41,52,66]. This can be explained by the laser energy; the higher power can generate more energy, as can lower scan speed.

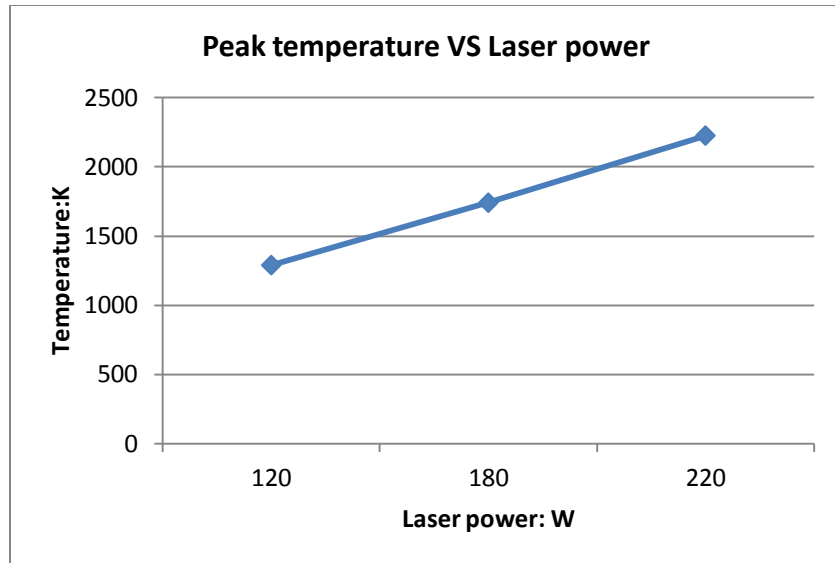


Figure 8 The influence of the laser power to peak temperature

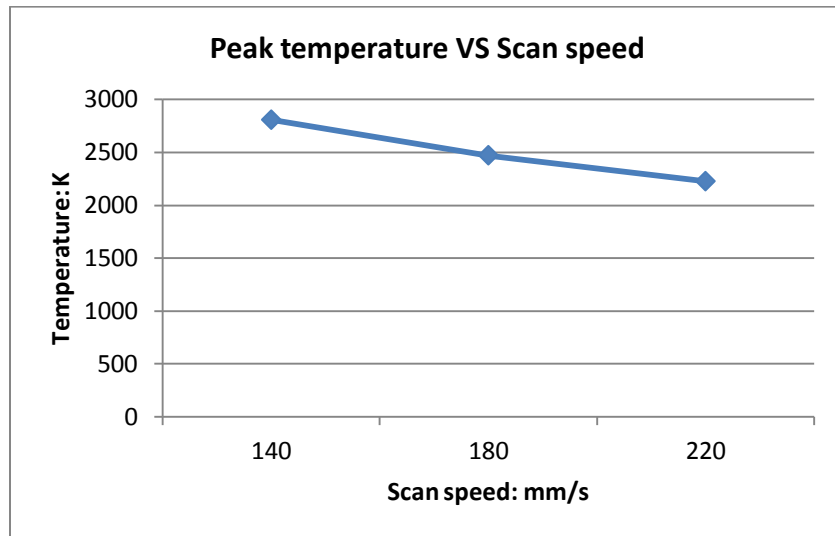


Figure 9 The influence of scan speed to peak temperature

Conclusion and future discussion

A comprehensive literature review of the thermal modeling method in laser sintering is presented in this paper. Classical Fourier heat transfer equations are the most common for describing the temperature distribution. Based on the Fourier equation, various models have been developed by combing latent heat, material thermal property nonlinearity, laser heat source distribution and interaction between a laser beam and powder bed[21,22,23,24,25,26,27]. Many models consider the influence of sintered part shrinkage, molten pool liquid flow and binding mechanism [32,33,34,35,36,37,74]. None of these models can be completely solved analytically. Numerical methods are employed extensively to solve the temperature distribution problem where the FE method has proven to be reliable using available commercial software. Finally, temperature measurement systems have been used to demonstrate the actual temperature distribution in SLM processes to compare against the models.

Great efforts have been put into the field of SLM thermal analysis since the emergence of SLM technology, but there are still many areas of improvement that are needed, including in analytical and simulation modeling as well as in the experimental measurement and control side. A better understanding of SLM sintering and binding mechanisms will lead to better modeling of the SLM thermal field. Better understanding of the input energy model, which includes laser beam distribution, energy penetration and material absorption ratio; and the thermal properties, such as thermal conductivity, density of powder before and after laser scanning, are needed.. From the literature review of various SLM thermal numerical models it can be seen that very few models attempt to represent parts in the same length scales as those which are built in SLM in reality. This is due to the fact that the problem is highly nonlinear, resulting in a heavy computational burden. Future work which carefully chooses an efficient numerical method and which utilizes some form of adaptive meshing technology will be of great help. With improvement in numerical modeling, the optimization of process parameters and exploration of empirical relationship between process parameters and temperature will become easier. These models can then be validated using well-developed temperature measurement systems. In the future, a parametric SLM simulation model which accurately predicts the optimal process parameters or parameter windows will significantly benefit users of laser sintering technology.

References

- [1] Gabriel Bugada Miguel Cervera, et al. (1999), "Numerical prediction of temperature and density distributions in selective laser sintering processes", *Rapid Prototyping Journal*, Vol. 5 Iss: 1 pp. 21 - 26
- [2] Gibson, L., Rosen, D., Stucker, B. (2009), "Additive manufacturing technologies: rapid prototyping to direct digital manufacturing", Springer, New York, NY
- [3] Nikolay K. Tolochko, et al. (2003), "Mechanisms of selective laser sintering and heat transfer in Ti powder", *Rapid Prototyping Journal*, Vol. 9 Iss: 5 pp. 314-326
- [4] X. C. Wang, T. Laoui, et al. (2002), "Direct Selective Laser Sintering of Hard Metal Powders: Experimental Study and Simulation", *Int J Adv Manuf Technol*, Vol.19 pp.351–357
- [5] J.P. Kruth, X. Wang, et al. (2003), "Lasers and materials in selective laser sintering", *Assembly Automation*, Vol. 23 Iss: 4 pp. 357 - 371
- [6] Simchi, A. (2006). "Direct laser sintering of metal powders: Mechanism, kinetics and microstructural features.", *Materials Science and Engineering: A* 428, Vol. 1 iss:2 pp.148-158.
- [7] Kolossov, S., E. Boillat, et al. (2004). "3D FE simulation for temperature evolution in the selective laser sintering process." *International Journal of Machine Tools and Manufacture*, Vol. 44 iss: 2-3 pp.117-123.
- [8] Zhang, D. Q., Q. Z. Cai, et al. (2010). "Select laser melting of W–Ni–Fe powders: simulation and experimental study." *The International Journal of Advanced Manufacturing Technology*, Vol. 51 iss:5-8 pp. 649-658.
- [9] Contuzzi, N., Campanelli, S.L., et al. (2011), "3d Finite element analysis in the selective laser melting process", *Int j simul model*, Vol. 10 iss:3 pp.113-121
- [10] Kruth, J. P., G. Levy, et al. (2007), "Consolidation phenomena in laser and powder-bed based layered manufacturing." *CIRP Annals - Manufacturing Technology*, Vol. 56 iss:2 pp. 730-759.

- [11] Levy, G. N., R. Schindel, et al. (2003). "Rapid Manufacturing and Rapid Tooling with Layer Manufacturing (Lm) Technologies, State of the Art and Future Perspectives." *CIRP Annals - Manufacturing Technology*, Vol.52 iss:2 pp. 589-609.
- [12] F. Miani, "Recent Developments Of Direct Metal Selective Laser Sintering", available at: <http://www.ics.trieste.it/media/133856/df143.pdf> (accessed 2 August 2012).
- [13] J.P. Kruth, B. Vandenbroucke, et al, "Benchmarking Of Different Sls/Slm Processes As Rapid Manufacturing Techniques", In *Int. Conf. Polymers & Moulds Innovations (PMI)*, Gent, Belgium, April 20-23, 2005
- [14] Sanjay Kumar(2003), "Selective Laser Sintering:A Qualitative and Objective Approach", *JOM Journal of the Minerals*, Vol.55, iss:10 pp.43-47
- [15] J.P. Kruth, X. Wang, et al. (2003), "Lasers and materials in selective laser sintering", *Assembly Automation*, Vol. 23 Iss: 4, pp.357 - 371
- [16] Roberts, I. A., C. J. Wang, et al. (2009), "A three-dimensional finite element analysis of the temperature field during laser melting of metal powders in additive layer manufacturing." *International Journal of Machine Tools and Manufacture*, Vol. 49 iss:12 pp. 916-923.
- [17] Fischer, P., V. Romano, et al. (2003). "Sintering of commercially pure titanium powder with a Nd:YAG laser source." *Acta Materialia*, Vol. 51 iss:6 pp. 1651-1662.
- [18] Singh, S. S., D. Roy, et al. (2009). "Studies on laser sintering of mechanically alloyed Al50Ti40Si10 composite." *Materials Science and Engineering*, Vol.501 iss:1 pp. 242-247.
- [19] H.S. Carslaw, J.C. Jaeger, (1959), "Conduction of Heat in Solids", Oxford University Press, Amen House, London E.C.4
- [2] Dai, K. and L. Shaw (2005). "Finite element analysis of the effect of volume shrinkage during laser densification." *Acta Materialia*, Vol. 53 iss:18 pp. 4743-4754.
- [21] Li Jianguai, Shi Yusheng, et al. (2008), "Numerical Simulation of Transient Temperature Field in Selective Laser Melting", *China Mechanical Engineering*, Vol 19 iss:20 pp.2492,-2495
- [22] Wei Jiang, K.W. Dalgarno et al. "Finite Element Analysis of Residual Stresses and Deformations in Direct Metal SLS Process", available at: <http://edge.rit.edu/content/P10551/public/SFF/SFF%202002%20Proceedings/2002%20SFF%20Papers/38-Jiang.pdf> (accessed 2 August 2012).
- [23] Zhang, D. Q., Q. Z. Cai, et al. (2010). "Select laser melting of W–Ni–Fe powders: simulation and experimental study." *The International Journal of Advanced Manufacturing Technology* Vol. 51 iss5 pp. 649-658.
- [24] Baojun ZHAO, Fazhong Shi, (2002), "Modeling of Selective Laser Sintering for PC Powder", *Journal of Beijing University of Aeronautics and Astronautics*, Vol.28 iss:6 pp.660-663
- [25] Shen Yifu, Gu Dongdong, et al. (2005), "Simulation of Temperature Field in Direct Metal Laser Sintering Processes", *China Mechanical Engineering*, Vol.16 iss:1 pp.67-73
- [26] Xing Jian, Sun Xiaogang, et al. (2011), "Simulation and testing of the transient temperature field of infrared laser sintering", *Journal of Harbin Engineering University*, Vol.32 iss:7 pp.965-968
- [27] Xing Jian, Sun Xiaogang, et al. (2009), "Simulation and testing of the transient temperature field of infrared laser sintering", *Acta Photonica Sinica*, Vol.38 iss:6 pp.1327-1330
- [28] Gusarov, A. V., I. Yadroitsev, et al. (2007). "Heat transfer modelling and stability analysis of selective laser melting." *Applied Surface Science* 254(4): 975-979.
- [29] Li, C., Y. Wang, et al. (2010). "Three-dimensional finite element analysis of temperatures and stresses in wide-band laser surface melting processing." *Materials & Design* 31(7): 3366-3373.

- [30]Shuai, C., P. Feng, et al. (2012). "Simulation of dynamic temperature field during selective laser sintering of ceramic powder." *Mathematical and Computer Modelling of Dynamical Systems*, Vol.1 iss:11
- [31]C.Chan, J.Mazumder, et al.(1984), "A two-dimensional Transient model for convection in laser melting pool", *Metallurgical Transactions A*, Vol. 15App.1984-2175
- [32]Chen, T. and Y. Zhang (2006). "Thermal modeling of laser sintering of two-component metal powder on top of sintered layers via multi-line scanning." *Applied Physics A*, Vol.86 iss:2 pp. 213-220.
- [33]Xiao, B. and Y. Zhang (2007). "Laser sintering of metal powders on top of sintered layers under multiple-line laser scanning." *Journal of Physics D: Applied Physics*, Vol. 40 iss:21 pp. 6725-6734.
- [34]Chen, T. and Y. Zhang (2004). "Numerical Simulation of Two-Dimensional Melting and Resolidification of a Two-Component Metal Powder Layer in Selective Laser Sintering Process." *Numerical Heat Transfer, Part A: Applications* 46(7): 633-649.
- [35]Yuwen Zhang, Amir Faghri.(1999), "Melting of a subcooled mixed powder bed with constant heat flux heating", *International Journal of Heat and Mass Transfer*, Vol.42, pp.775-788
- [36]Yuwen Zhang, A.Faghri, et al.(2000), "Three-Dimensional Sintering of Two-Component Metal Powders With Stationary and Moving Laser Beams", *Transactions of the ASME*, Vol.122 pp.150-158
- [37]Xiao, B. and Y. Zhang (2007). "Marangoni and Buoyancy Effects on Direct Metal Laser Sintering with a Moving Laser Beam." *Numerical Heat Transfer, Part A: Applications* , Vol.51 iss:8 pp.715-733.
- [38]Gusarov, A. V. and J. P. Kruth (2005). "Modelling of radiation transfer in metallic powders at laser treatment." *International Journal of Heat and Mass Transfer* 48(16): 3423-3434.
- [39]F. Niebling, A. Otto, et al. "Analyzing The Dmls-Process By A Macroscopic Fe-Model", available at:
<http://utwired.engr.utexas.edu/lff/symposium/proceedingsArchive/pubs/Manuscripts/2002/2002-43-Niebling.pdf>(accessed 2 August 2012).
- [40]M. Shiomi, A. Yoshidome, et al.(1999), "Finite element analysis of melting and solidifying processes in laser rapid prototyping of metallic powders", *International Journal of Machine Tools & Manufacture*, Vol39 pp.237-252
- [41]Zhang Jian, Li Deying et al. "Simulation of Temperature Field in Selective Laser Sintering of Copper Powder", available at:
<http://ieeexplore.ieee.org/stamp/stamp.jsp?arnumber=05535715>(accessed 2 August 2012).
- [42]Song, B., S. Dong, et al. (2011). "Process parameter selection for selective laser melting of Ti6Al4V based on temperature distribution simulation and experimental sintering." *The International Journal of Advanced Manufacturing Technology* 61(9-12): 967-974.
- [43]Chen, W.-L., Y.-C. Yang, et al. (2007). "Estimating the absorptivity in laser processing by inverse methodology." *Applied Mathematics and Computation* 190(1): 712-721.
- [44]F. Thummler, R. Oberacker, "An Introduction to Powder Metallurgy", The University Press, Cambridge, London, 1993.
- [45]M. Rombouts, et al., " Light extinction in metallic powder beds: correlation with powder structure", *Journal of Applied Physics* , Vol.98 iss: 1.
- [46]T.W.Eagar, N.S.Tasi,(1983). "Temperature fields produced by traveling distributed heat sources", *welding research supplement*, pp.346-355,

- [47] John Michael Dowden, (2001), "The Mathematics of Thermal Modeling: An Introduction to The Theory Of Laser Material Processing", CHAPMAN & HALL/CRC, London
- [48] M. LABUDOVIĆ, (2003), "A three dimensional model for direct laser metal powder deposition and rapid prototyping", *Journal Of Materials Science*, Vol. 38 pp.35– 49
- [49] Li JunChang, C. Langlade a, et al. (1999), "Evaluation of the thermal field developed during pulsed laser treatments: semi analytical calculation", *Surface and Coatings Technology*, Vol.115 pp. 87–93
- [50] M. Matsumoto, M. Shiomi, et al. (2002), "Finite element analysis of single layer forming on metallic powder bed in rapid prototyping by selective laser processing", *International Journal of Machine Tools & Manufacture*, Vol. 42 pp.61–67
- [51] Patil, R. B., V. Yadava (2007). "Finite element analysis of temperature distribution in single metallic powder layer during metal laser sintering." *International Journal of Machine Tools and Manufacture* 47(7-8): 1069-1080.
- [52] Yin, J., H. Zhu, et al. (2012). "Simulation of temperature distribution in single metallic powder layer for laser micro-sintering." *Computational Materials Science* 53(1): 333-339.
- [53] Ameer K. ibraheem, Brian Derby, et al. (2003), "Thermal and Residual Stress Modelling of the Selective Laser Sintering Process", *Materials Research Society*, Vol.758 pp.47-52
- [54] John D. Williams, Carl R. Deckard, (1998), "Advances in modeling the effects of selected parameters on the SLS process", *Rapid Prototyping Journal*, Vol. 4 Iss: 2 pp. 90 - 100
- [55] E. Magenes, R.H.Nochetto, et al. (1987), "Energy error estimates for a linear scheme to approximate nonlinear parabolic problems", *Mathematical modeling and numerical analysis*, Vol.21 pp.655-678
- [56] Bai, P.-k., J. Cheng, et al. (2006). "Numerical simulation of temperature field during selective laser sintering of polymer-coated molybdenum powder." *Transactions of Nonferrous Metals Society of China*, Vol.16 pp.603-607.
- [57] Laurent Van Belle, Guillaume Vansteenkiste, et al. "Comparisons of numerical modelling of the Selective Laser Melting", <http://www.scientific.net/KEM.504-506.1067>
- [58] A. Wegner and G. Witt, (2011), "Process Monitoring In Laser Sintering Using Thermal Imaging", available at: <http://utwired.engr.utexas.edu/lff/symposium/proceedingsArchive/pubs/Manuscripts/2011/2011-30-Wegner.pdf> (accessed 2 August 2012).
- [59] Fischer, P., M. Locher, et al. (2004). "Temperature measurements during selective laser sintering of titanium powder." *International Journal of Machine Tools and Manufacture* 44(12-13): 1293-1296.
- [60] Qiu Jiangguo, (2003), "Measurement of temperature field during laser sintering of polymer-coated metal powder", *Chinese Journal of Scientific Instrument*, Vol.24 iss:4 pp.54-55
- [61] Dong, L., A. Makradi, et al. (2009). "Three-dimensional transient finite element analysis of the selective laser sintering process." *Journal of Materials Processing Technology* 209(2): 700-706.
- [62] J.-P. Kruth, P. Mercelis, et al. "Feedback control of Selective Laser Melting", available at: <https://lirias.kuleuven.be/bitstream/123456789/185342/1> (accessed 2 August 2012).
- [63] Craeghs, T., F. Bechmann, et al. (2010). "Feedback control of Layerwise Laser Melting using optical sensors." *Physics Procedia*, Vol 5 pp. 505-514.
- [64] Berumen, S., F. Bechmann, et al. (2010). "Quality control of laser- and powder bed-based Additive Manufacturing (AM) technologies." *Physics Procedia*, Vol. 5 pp. 617-622.

- [65]Chivel, Y. and I. Smurov (2010). "On-line temperature monitoring in selective laser sintering/melting." *Physics Procedia* 5: 515-521.
- [66]Childs, T. H. C., C. Hauser, et al. (2004). "Mapping and Modelling Single Scan Track Formation in Direct Metal Selective Laser Melting." *CIRP Annals - Manufacturing Technology* 53(1): 191-194.
- [67]C. Hauser, T.H.C. Childs, et al. "Further Developments In Process Mapping And Modelling In Direct Metal Selective Laser Melting", available at: <http://utwired.engr.utexas.edu/lff/symposium/proceedingsArchive/pubs/Manuscripts/2004/2004-45-Hauser.pdf>(accessed 2 August 2012).
- [68]Singh, A. K. and R. S. Prakash (2010). "Response surface-based simulation modeling for selective laser sintering process." *Rapid Prototyping Journal* 16(6): 441-449.
- [69]Chatterjee, A. N., S. Kumar, et al. (2003). "An experimental design approach to selective laser sintering of low carbon steel." *Journal of Materials Processing Technology* 136(1-3): 151-157.
- [70]M. Averyanova, E. Cicala, et al. (2012), "Optimization of Selective Laser Melting technology using design of experiments method, Innovative Developments in Virtual and Physical Prototyping", in *Proceedings of the 5th International Conference on Advanced Research in Virtual and Rapid Prototyping*, Leiria, Portugal, 28 September - 1 October, 2011,459–466
- [71]M. Averyanova, E. Cicala, et al. (2012), "Experimental design approach to optimize selective laser melting of martensitic 17-4 PH powder: part I - single laser tracks and first layer", *Rapid Prototyping Journal*, Vol. 18 Iss: 1 pp. 28 - 37
- [72]Ning, Y., J. Y. H. Fuh, et al. (2004). "An intelligent parameter selection system for the direct metal laser sintering process." *International Journal of Production Research* 42(1): 183-199.
- [73]E Boillat¹, S Kolosov¹, et al. (2004), "Finite element and neural network models for process optimization in selective laser sintering", in *Proceeding of . Instn Mech. Engrs Part B: J. Engineering Manufacture*, Vol. 218 pp.1-8
- [74]Konrad, C., Y. Zhang, et al. (2005). "Analysis of melting and resolidification in a two-component metal powder bed subjected to temporal Gaussian heat flux." *International Journal of Heat and Mass Transfer* 48(19-20): 3932-3944.
- [75]J. C. Nelson, N. K. Vail, et al. "Laser Sintering Model for Composite Materials", available at: <http://utwired.engr.utexas.edu/lff/symposium/proceedingsArchive/pubs/Manuscripts/1993/1993-41-Nelson.pdf>(accessed 2 August 2012).